

$T = \frac{5}{2}$   $^{27}\text{Na}$  from  $^{14}\text{C} + ^{14}\text{C}$ , and the  $N = 16$  shell gap

M. W. Cooper, S. L. Tabor, T. Baldwin, D. B. Campbell, C. Chandler, C. R. Hoffman, K. W. Kemper, J. Pavan, A. Pipidis, M. A. Riley, and M. Wiedeking

*Department of Physics, Florida State University, Tallahassee, Florida 32306*

(Received 14 December 2001; published 17 April 2002)

For the first time a comprehensive level and decay scheme has been obtained for a  $T = \frac{5}{2}$  nucleus in the  $s$ - $d$  shell ( $^{27}\text{Na}$ ) by using a radioactive beam and target. Particle- $\gamma$  and  $p$ - $\gamma$ - $\gamma$  coincidences were measured following the  $^{14}\text{C}(^{14}\text{C}, p\gamma)^{27}\text{Na}$  reaction at  $E_{\text{lab}} = 22$  MeV. The results do not support an inversion of the  $2s_{1/2}$  and  $1d_{5/2}$  orbitals, as previously proposed for  $T_z \geq 3$ , but they do suggest an increased  $N = 16$  gap between the  $2s_{1/2}$  and  $1d_{3/2}$  orbitals due to the neutron excess. A consistent interpretation of the level scheme in terms of the  $s$ - $d$  shell model using the USD Hamiltonian is possible below 4 MeV, but differences increase at higher excitation energies. Another interpretation is that the influences of both the  $p_{1/2}$  and  $f_{7/2}$  intruder orbitals increase simultaneously with increasing  $T$ , an effect not included in the USD Hamiltonian.

DOI: 10.1103/PhysRevC.65.051302

PACS number(s): 27.30.+t, 21.10.Pc, 23.20.Lv, 25.60.-t

The development of large-basis shell model calculations has greatly improved the description of the structure of nuclei in the  $s$ - $d$  shell, particularly with the use of the USD Hamiltonian of Brown and Wildenthal [1]. These calculations have been quite successful over a wide range of spins including the rotational bands near the middle of the  $s$ - $d$  shell [2,3]. In fact they predicted very well the recently observed first  $10^+$  level in  $^{24}\text{Mg}$  [4].

Although the USD Hamiltonian has been fitted and tested over a wide range of spins, the same is not true for isospin. The vast preponderance of the measured levels used to determine the USD Hamiltonian were taken from nuclei with nearly equal numbers of neutrons and protons [5]. Only a very few  $T = 2$  levels and no  $T = \frac{5}{2}$  excited states were included in the fit. Likewise, few experimental tests have been made of the model predictions for higher isospin, although the need for reliable models for the structure of nuclei far from stability will be extremely important for future radioactive beam facilities.

An important question in this regard is how the shell structure changes with isospin. The  $N = 20$  shell gap was shown to disappear in neutron-rich  $^{32}\text{Mg}$  [6,7], and a new shell gap at  $N = 16$  has been proposed for  $T_z \geq 3$  [8]. The origin of the new magic number may lie in neutron halo formation which lowers the energy of low-angular momentum orbitals such as  $s_{1/2}$ , leading, for example, to the abnormal  $\frac{1}{2}^+$  ground state of  $^{15}\text{C}$ . Evidence for just such an increase in neutron skin thickness with increasing neutron number across the Na and Mg isotopes has been presented [9,10]. Another indication of a possible shell closure at  $N = 16$  is the nearly spherical ( $Q = -7.2$  mb) ground state (g.s.) of  $T = \frac{5}{2}$   $^{27}\text{Na}$  [11] surrounded by more deformed prolate shapes for  $N < 16$  and  $N > 16$ .

To investigate the effects of an emerging shell gap, as well as of other possible high-isospin phenomena, on the structure of an  $N = 16$  nucleus, we have used a neutron-rich  $^{14}\text{C}$  beam and target in conjunction with a modern  $\gamma$  detection array to study  $^{27}\text{Na}$ . It has led to the first detailed  $\gamma$  decay scheme for a  $T = \frac{5}{2}$  nucleus in the  $s$ - $d$  shell. Previously, only a few excited states had been observed in  $^{27}\text{Na}$

using the  $^{26}\text{Mg}(^{18}\text{O}, ^{17}\text{F})$  reaction [12,13]. Lack of knowledge of the spins, decay modes, or reaction selectivity prevented any reliable identification of these levels with model predictions.

In the present work, particle- $\gamma$  coincidences were measured from the reaction of a radioactive, albeit long-lived,  $^{14}\text{C}$  beam on a  $^{14}\text{C}$  target. The  $^{14}\text{C}$  beam was produced by sputtering Cs from an enriched  $\text{Fe}_3\text{C}$  sample [14] in a dedicated, removable ion source. Because oscillatory structure has been seen in the elastic scattering of  $^{14}\text{C}$  on  $^{14}\text{C}$  [15], several beam energies from 18 to 33 MeV were explored. An energy of  $E_{\text{lab}} = 22$  MeV was chosen for the production measurement, because it led to the most favored population of  $^{27}\text{Na}$ . A beam current of about 5 pA was incident on the  $600 \mu\text{g}/\text{cm}^2$  self-supporting enriched  $^{14}\text{C}$  target for a running time of 18 d.

Charged particles from the reaction were detected and identified using a Si detector telescope consisting of a  $5000 \mu\text{m}$   $E$  detector and a  $150 \mu\text{m}$   $\Delta E$  detector placed at  $0^\circ$  relative to the beam and subtending  $0.82$  sr of solid angle. A  $27 \text{ mg}/\text{cm}^2$  Au foil was placed between the target and detector to stop the  $^{14}\text{C}$  beam. Three Compton-suppressed clover detectors and one Compton-suppressed high purity germanium detector (HPGe) were placed at  $90^\circ$  relative to the beam to measure coincident  $\gamma$  rays. Six more suppressed HPGe detectors were placed at  $35^\circ$  and  $145^\circ$ . Add-back mode was used in the analysis of the clover detectors to improve their efficiency for higher-energy  $\gamma$  rays.

The reaction was entirely dominated by two-neutron emission back to stable  $^{26}\text{Mg}$ .  $\gamma$  decays could be seen for the first time in  $^{27}\text{Na}$  only by gating on the weak ( $< 0.1\%$ ) proton emission channel. Examples of  $\gamma$  spectra in coincidence with protons are shown in Fig. 1. In order to avoid misidentifying  $^{25}\text{Na}$  lines [from  $^{12}\text{C}(^{14}\text{C}, p)$  due to a small  $^{12}\text{C}$  target contamination] and  $^{26}\text{Na}$  lines (from  $^{27}\text{Na} \rightarrow n + ^{26}\text{Na}$ ) as  $^{27}\text{Na}$  ones, both the  $t$ - $\gamma$  and  $d$ - $\gamma$  coincidence spectra were carefully examined to identify all  $^{25,26}\text{Na}$   $\gamma$  decays.

The primary information for the placement of  $^{27}\text{Na}$  lines in the level scheme comes from the energies of the protons in

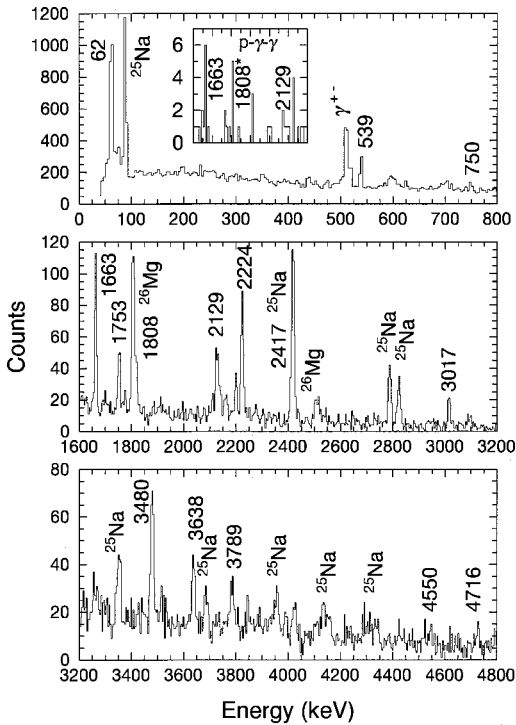


FIG. 1. Portions of the  $\gamma$  spectrum in coincidence with protons. Part of the  $p$ - $\gamma$ - $\gamma$  spectrum gated by the 62 keV transition is shown in the inset.

coincidence with them. This determines the excitation energy of the parent state of a  $\gamma$  line to a few hundred keV, limited by straggling in the Au beam stop foil, kinematic broadening from the large particle detector solid angle, and low statistics. Some examples of proton spectra in coincidence with  $\gamma$  lines are shown in Fig. 2. The highest proton energy corresponds to the excitation of the state emitting that  $\gamma$  transi-

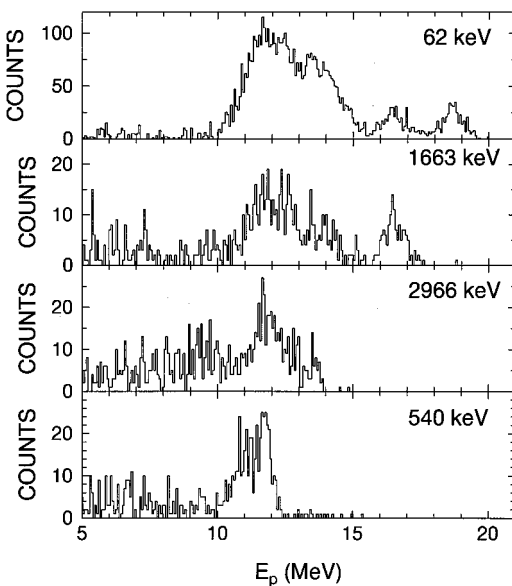


FIG. 2. Proton spectra in coincidence with individual  $\gamma$  lines in  $^{27}\text{Na}$ .

tion.  $p$ - $\gamma$ - $\gamma$  coincidences would be invaluable in building the level scheme, but only a few could be seen because of the weakness of the reaction leading to  $^{27}\text{Na}$ .  $p$ - $\gamma$ - $\gamma$  coincidences with the 62 keV transition are shown in the inset of Fig. 1. Coincidences were also seen between the 539 and 2129 keV lines. Further valuable evidence for placement in the level scheme comes from the multiple decay paths adding to the same excitation energy.

The level and decay scheme for  $^{27}\text{Na}$  deduced from the present work is shown in Fig. 3. The levels inferred from the previous ( $^{18}\text{O}$ ,  $^{17}\text{F}$ ) reactions are shown on the left side. Both experiments observed a peak which corresponds to the 2191–2224 keV doublet. Other likely correspondences are 1720–1725 keV, 1860–1815 keV, and 3820–3837 keV. No further evidence has been seen for the 800(100) keV peak [12]. Because of the limited resolution in the particle channel, it was not possible to determine to which member of the g.s. doublet decays proceeded in the absence of other information, such as  $p$ - $\gamma$ - $\gamma$  coincidences or energy sums. Such decays are shown on the right side of the level scheme with the g.s. doublet as one broad destination.

A spin of  $\frac{3}{2}^+$  was determined for the ground state (g.s.) from laser spectroscopy of the atomic  $D_1$  line [16]. Positive parity was established by the observation of allowed  $\beta$  decays to the  $\frac{3}{2}^+$  and  $\frac{5}{2}^+$  states in  $^{27}\text{Mg}$  [17–19]. The relatively strong 62 keV line and its coincident proton energy prove the existence of a 62 keV level which could not have been resolved in the ( $^{18}\text{O}$ ,  $^{17}\text{F}$ ) reactions. This level appears analogous to the 90 keV  $\frac{3}{2}^+$  state in  $^{25}\text{Na}$ . The g.s. doublet can be understood from the couplings of three  $d_{5/2}$  protons. Based on the lowest  $0^+$ ,  $2^+$ , and  $4^+$  states in the nearest known two-proton system,  $^{24}\text{Ne}$ , this leads to  $\frac{5}{2}^+$ ,  $\frac{3}{2}^+$ , and  $\frac{9}{2}^+$  states at 0, 48, and 3017 keV, respectively [20]. The full USD shell model calculations also predict a  $\frac{5}{2}^+$  ground state and a 14 keV  $\frac{3}{2}^+$  level. Altogether, these make an assignment of  $\frac{3}{2}^+$  to the 62 keV level quite certain.

Beyond the g.s. doublet,  $J^\pi$  assignments become weaker. Further comparisons with neighboring  $^{25}\text{Na}$  do not help because it is poorly known and the structure changes too fast with  $N$ . The observed  $\gamma$  decays provide spin limitations, and a few two-point angular distributions could be measured with the limited statistics available. These are shown in Fig. 4 along with typical theoretical ones for the spins given in Fig. 3. They show that the angular distribution for the 1663 keV line is isotropic and those for the 2129 and 2224 keV (62 keV) lines are consistent with  $E2$  ( $M1$ ) decay. Other spin suggestions will be discussed below based on model comparisons.

Shell model calculations using OXBASH [21] with the USD interaction [1] provide some interpretation of the structure of  $^{27}\text{Na}$ . The calculated levels are shown on the right side of Fig. 3. Only higher spin states are shown at higher excitation energies for clarity. Suggested correspondences with experimental states are listed in Table I, as discussed below.

Above the g.s. doublet, three states are predicted around 2 MeV, but four were observed. Three of the experimental states decay to the  $\frac{3}{2}^+$  level and cannot have spins above  $\frac{7}{2}^+$ .

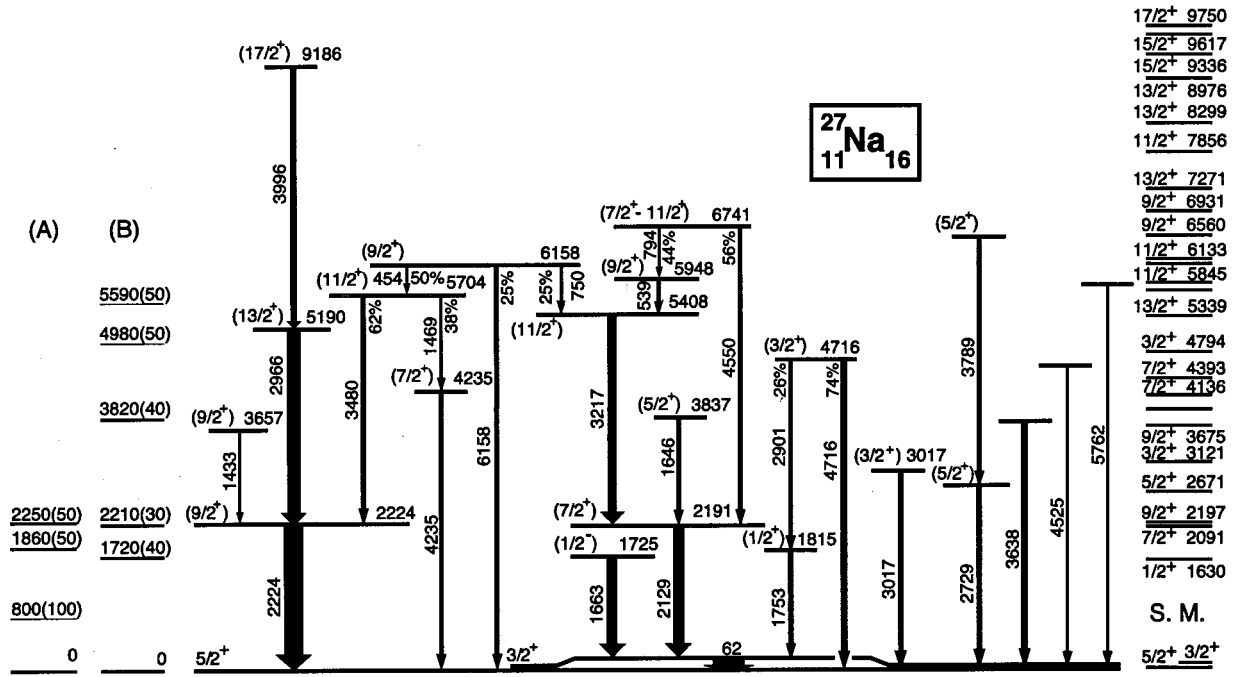


FIG. 3. Level and decay scheme of  $^{27}\text{Na}$  based on the present work. Previously reported levels are shown in columns A [12] and B [13], while shell model predictions are on the right. The widths of the transition arrows are proportional to their intensities.

This leaves the 2224 keV state as the only candidate to correspond to the predicted  $\frac{9}{2}^+$  level at 2197 keV. Both the number of higher lying states which decay to the 2191 keV level and the proximity in energy favor identification with the predicted  $\frac{7}{2}^+$  state at 2091 keV. Of the remaining 1725 and 1815 keV levels, one could be the predicted  $\frac{1}{2}^+$  state at 1630 keV and the other may be an intruder. In a companion study to Ref. [13], it was shown [22] that the ( $^{18}\text{O}, ^{17}\text{F}$ ) reaction populates  $\pi p_{1/2}$  hole states well, so the 1725 keV level seen in Ref. [13] may be the  $\frac{1}{2}^-$  intruder state. The corresponding state lies at 2.64 MeV in  $^{23}\text{Na}$ , but is not known in  $^{25}\text{Na}$ . This would leave the 1815 keV level as the predicted  $\frac{1}{2}^+$  state. The opposite parity assignment to the two spin  $\frac{1}{2}$  states is also possible.

The next two states predicted by the shell model,  $\frac{5}{2}^+$  at 2671 keV and  $\frac{3}{2}^+$  at 3121 keV, may correspond to the parents of the 2729 and 3017 keV decays. Above this, more states are predicted than have been observed, and  $\gamma$  decay patterns become more important in identifying states. For instance, the preferential decay of the 3657 keV level to the

TABLE I. Suggested comparisons between observed energy levels in  $^{27}\text{Na}$  and those predicted by the  $s$ - $d$  shell model using the USD interaction.

SM $E_x$ (keV)	SM $J^\pi$	Exp. $E_x$ (keV)	(SM - Exp) (keV)
0	$5/2^+$	0.0	0
14	$3/2^+$	62	-48
1630	$1/2^+$	1815	-185
2091	$7/2^+$	2191	-100
2197	$9/2^+$	2224	-27
2671	$5/2^+$	2729 <sup>a</sup>	-58
3121	$3/2^+$	3017 <sup>a</sup>	104
3675	$9/2^+$	3657	18
3923	$5/2^+$	3837	86
4393	$7/2^+$	4235	158
4795	$3/2^+$	4716	79
5339	$13/2^+$	5190	149
5845	$11/2^+$	5408	437
6133	$11/2^+$	5704	429
6211	$5/2^+$	6518 <sup>a</sup>	-307
6560	$9/2^+$	5948	608
6931	$9/2^+$	6158	773
9750	$17/2^+$	9186	564

<sup>a</sup>Level excitation energy may be 62 keV higher.

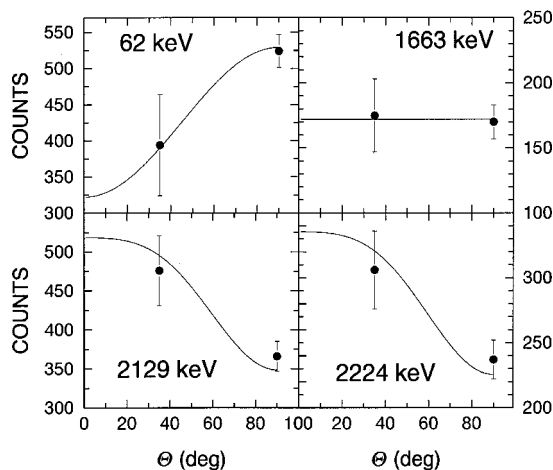


FIG. 4. Two point angular distributions of transitions in  $^{27}\text{Na}$ . The lines indicate isotropic and typical  $M1$  and  $E2$  angular distributions.

$\frac{9}{2}^+$  state suggests a moderately high spin and probable identification with the predicted second  $\frac{9}{2}^+$  state at 3675 keV, for which a 68% decay branch to the first  $\frac{9}{2}^+$  state is predicted.

A number of low energy decays occur among a group of levels between 5408 and 6741 keV where higher energy decays to lower lying levels would be energetically favored. Generally similar decay patterns are predicted for a group of shell model states, and the suggested identifications are based on the decay pattern correspondences, rather than energy correspondences, because the decays are so distinctive. As a result, the predicted energies are several hundred keV higher than the observed ones. There are predicted states close in energy to the observed ones, but not with strong, low-energy decays.

Protons in coincidence with the 3996 keV line imply an excitation energy far above the neutron decay threshold of 6.75 MeV, and penetrability calculations show that states of spin less than  $\frac{17}{2}\hbar$  would decay almost entirely by neutron emission. This leads to an identification with the  $\frac{17}{2}^+$  shell model state predicted at 9750 keV. A  $\frac{17}{2}^+$  state would decay to the  $\frac{13}{2}^+$  state, for which the 5190 keV level is the best candidate. This yrast sequence, with some resemblance to a rotational band, drops below the shell model predictions, perhaps due to increasing influences of the  $f_{7/2}$  shell.

In summary, the level scheme of  $^{27}\text{Na}$  shows that the  $2s_{1/2}$  orbital has not dropped below the  $1d_{5/2}$  one at  $T = \frac{5}{2}$  since the g.s. doublet is well explained by the coupling of  $d_{5/2}$  protons in both the simple proton-only coupling model and in the full USD shell model calculations. The lowest  $\frac{1}{2}^+$  state lies at 1815 or possibly 1725 keV. However, the  $2s_{1/2}$  orbital may have dropped enough to create a significant shell gap at  $N$

$=16$ . The nearly spherical shape implied by the measured quadrupole moment and the lack of good rotational structure in Fig. 3 at lower energies provide evidence for an  $N=16$  gap. Further support comes from the measured positions of the lowest  $\frac{5}{2}^+$ ,  $\frac{3}{2}^+$ , and  $\frac{9}{2}^+$  states in  $^{27}\text{Na}$  which imply [20]  $2^+$  and  $4^+$  states at 1484 and 2924 keV in  $T=3$ ,  $N=16$   $^{26}\text{Ne}$ . This is a perfect vibrational spacing, consistent with spherical shape and a shell gap at  $N=16$ .

A consistent interpretation is possible for the first 4 MeV of excitation of  $^{27}\text{Na}$  within the shell model using the USD interaction if one of the states is a  $\pi p_{1/2}$  intruder hole state. At higher energies either the predicted energies or decay patterns do not agree as well with experiment as for nuclei with smaller  $T$ . This could be an indication that the reduced neutron binding and increased radius introduces new physics such as a widening shell gap at  $N=16$ , especially if the intruder state lies higher. Or the larger deviations at higher energies could result from an increasing influence  $\nu f_{7/2}$  configurations. If so, then the effect of higher isospin is that both the lower  $p_{1/2}$  shell and the higher  $f_{7/2}$  shell become important simultaneously as  $Z$  approaches the former and  $N$ , the latter, an effect that is not included in the USD interaction based on low  $T$  nuclei. In any case, further detailed studies of high  $T$  nuclei promise new insights into the role of shell gaps in nuclear structure.

The work was supported in part by the U.S. National Science Foundation. We are grateful to V. Griffin, E. G. Myers, and B. G. Schmidt for their work on the radioactive  $^{14}\text{C}$  ion source and to J. Janecke, V. G. Goldberg, and P. Barber for their contributions to the  $^{14}\text{C}$  targets.

- 
- [1] B.A. Brown and B.H. Wildenthal, *Annu. Rev. Nucl. Part. Sci.* **38**, 29 (1988).  
 [2] R.K. Sheline *et al.*, *J. Phys. G* **14**, 1201 (1988).  
 [3] D.M. Headley *et al.*, *Phys. Lett. B* **198**, 433 (1988).  
 [4] I. Wiedenhöver *et al.*, *Phys. Rev. Lett.* **87**, 142502 (2001).  
 [5] B.H. Wildenthal, M.S. Curtin, and B.A. Brown, *Phys. Rev. C* **28**, 1343 (1983).  
 [6] D. Guillemaud-Mueller *et al.*, *Nucl. Phys.* **A426**, 37 (1984).  
 [7] T. Motobayashi *et al.*, *Phys. Lett. B* **346**, 9 (1995).  
 [8] A. Ozawa *et al.*, *Phys. Rev. Lett.* **84**, 5493 (2000).  
 [9] T. Suzuki *et al.*, *Phys. Rev. Lett.* **75**, 3241 (1995).  
 [10] T. Suuki *et al.*, *Nucl. Phys.* **A630**, 661 (1998).  
 [11] M. Keim *et al.*, *Eur. Phys. J. A* **8**, 31 (2000).  
 [12] I. Paschopoulos *et al.*, *Phys. Rev. C* **18**, 1277 (1978).  
 [13] L.K. Fifield *et al.*, *Nucl. Phys.* **A437**, 141 (1985).  
 [14] R. Maier *et al.*, *Nucl. Instrum. Methods* **155**, 55 (1978).  
 [15] D.M. Drake *et al.*, *Phys. Lett.* **95B**, 36 (1981).  
 [16] G. Huber *et al.*, *Phys. Rev. C* **18**, 2342 (1978).  
 [17] D.E. Alburger, D.R. Goosman, and C.N. Davids, *Phys. Rev. C* **8**, 1011 (1973).  
 [18] E. Roeckl *et al.*, *Phys. Rev. C* **10**, 1181 (1974).  
 [19] C. Détraz *et al.*, *Phys. Rev. C* **19**, 164 (1979).  
 [20] Kris L. G. Heyde, *The Nuclear Shell Model* (Springer-Verlag, Berlin, 1994), p. 121.  
 [21] B.A. Brown, A. Etchegoyen, and W.D.M. Rae, *The Oxford-Buenos Aires-MSU Shell Model Code*, Technical Report MSUCL No. 524, 1988.  
 [22] N.A. Orr *et al.*, *Nucl. Phys.* **A491**, 457 (1989).